

ISSN 0252-1075

Research Report No. RR-056

Contributions from  
Indian Institute of Tropical Meteorology

RR-56  
2.11.93

AN EXPERIMENTAL SET-UP TO  
ESTIMATE THE HEAT BUDGET NEAR  
THE LAND SURFACE INTERFACE

by

K.G. VERNEKAR, SANGEETA SAXENA,  
J.S. PILLAI, B.S. MURTHY, T. DHARMARAJ,  
AND BRIJ MOHAN

PUNE - 411 008  
INDIA  
JULY 1993

An experimental set-up to estimate the heat budget  
near the land surface interface

K G Vernekar, Sangeeta Saxena, J S Pillai, B S Murthy,  
T. Dharmaraj and Brij Mohan

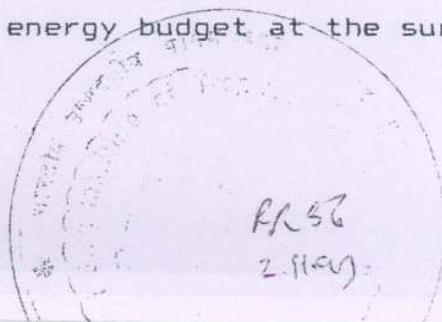
Indian Institute of Tropical Meteorology, Pune 411 008

1. Introduction

The study of interaction between land-surface and the atmosphere is important for the estimation of energy budget near the land surface. The contribution of the fluxes of heat, moisture and momentum at the surface help in understanding the land-surface processes. There is a growing interest in these parameters as they define the mean profiles near the surface and the atmospheric boundary layer and ultimately determine the steady state reached by the atmosphere.

In order to study the energy budget and the turbulent transfer of energy at the surface, observational techniques are required for direct measurement and constant monitoring of dry and wet-bulb temperature, horizontal and vertical wind and radiation, at a fast rate. With this objective in view, an experimental set-up has been designed with the required sensors and instrumentation and an experiment has been conducted at IITM campus, Pashan, Pune.

In this report, details of the experimental set-up are given. The data acquired through this experimental set-up over a period of two weeks has been presented. Also, the initial results from the preliminary analysis of the energy budget at the surface are presented.



## 2. Observation site

The experiment was conducted during 5 - 22 May 92 at IITM, Pashan campus, Pune ( $18^{\circ} 32'N$ ,  $73^{\circ} 51'E$ , 559m amsl). The observational site is flat and has dry, bare soil. The experimental area is surrounded by short, dry grass and there is a fetch to height ratio of 40, for the tallest tower used in the experiment. Figure 1 shows the schematic layout of the different towers and instruments used in the experiment.

## 3. Instrumentation details

Figure 2 shows the data acquisition set-up for the different sensors. Slow data from the soil temperature sensor, net radiometer and the flux plates are recorded continuously on an analog strip chart recorder. Fast data acquired from the dry-bulb and wet-bulb temperature towers and the wind speed tower are fed through a 12-channel data logger to a personal computer and the data are transferred to floppies. Similarly, data from the 3-axis Gill propeller anemometer are also acquired on floppies. Sonic anemometer is coupled through an RS-232 port of the PC and data are obtained on floppies. All the data are collected for 20 minutes at every hour.

### 3.1 Seven-level temperature recorder

A seven level temperature tower was designed and fabricated to study the temperature variations and profiles close to the surface. The levels are 5, 15, 20, 30, 40, 80 and 160 cms above ground surface.

Three-terminal linearized thermistors (2 mm diameter),

manufactured by M/s Yellow Springs Instrument, Co. (YSI), USA, are used as temperature sensors. Their sensitivity is 127.096 ohms/ °C when used in a resistance mode. To minimize errors due to cables etc, each thermistor is operated in a constant current circuit with 87.7  $\mu$ A current flowing through it. The voltage drop appearing across the thermistor due to its resistance variation is calibrated in terms of temperature. For a temperature range of 0 °C to 50 °C the output voltage varies linearly from 1066 mV to 512 mV giving a voltage change of 11.1 mV/°C. Figure 3 shows the variation in temperature for a day at 3 levels i.e. 5 cm, 30 cm and 160 cm.

### 3.2 2-level Wet bulb temperature tower

For humidity measurements, wet-bulb temperature sensors were mounted on a 1.6 m high tower, at 30 and 160 cm. Three terminal linearized YSI thermistors (2 mm dia.) were utilized as sensors and were operated in a resistance mode. A constant current of 75  $\mu$ A was allowed to flow through the thermistors and the output voltage variation due to change in thermistor resistance was calibrated in terms of temperature. For a temperature change from 0 °C to 50 °C, a linear voltage change from 897 mV to 430 mV was obtained giving a variation of 9.34 mV/°C. The wetting of the thermistor was done using a muslin cloth. Figure 4 shows the variations in the wet-bulb temperature at the two levels 30 and 160 cm for a day, on 20 May 1992.

### 3.3 3-level wind speed tower

Cup anemometers, designed and fabricated at the institute, were mounted on a 1.6 m high tower at 30, 80 and 160 cm. Infrared

light chopping arrangement was used to generate pulses which were then fed to a frequency to voltage conversion circuit so that a direct calibration of wind speed Vs voltage could be obtained. A mean calibration graph was used for all the three sensors and a linear output voltage was obtained from 0 mV to 500 mV (0 - 10 m/s). Figure 5 shows the wind speed variations for 20 May 1992 at the two levels i.e. 30 cm and 160 cm.

The analog outputs of the 7-level temperature tower, 3-level wind speed tower and the 2-level wet bulb temperature tower were fed through a 12-channel data logger to a PC and the data were recorded on floppies at pre-determined intervals. The data logger has a capability of recording at intervals ranging from 0.1 sec to 10 secs. In the present experiment the data were recorded at a rate of once every five seconds for a duration of 20 minutes at each hour.

#### 3.4 6-level soil temperature recorder

To study the temperature variations at the soil surface and below it, a six level soil temperature recorder has been developed. The temperature measurements were made at the levels : 10 cm above the surface, surface, and 10, 20, 30 and 60 cms below the surface. Figure 6 shows the cross-sectional view of the probe which can be inserted into the ground such that the second thermistor from the top just touches the earth's surface.

Four-terminal (YSI) linearized thermistors (3.16 mm diameter) were used as temperature sensors. They have a sensitivity of 129.163 ohms/°C when utilized in a resistance mode. Each thermistor is connected as the feedback resistance of

an operational amplifier. There are altogether six operational amplifiers, one each for the levels mentioned above. The outputs of these amplifiers are multiplexed and then compared in sequence with a known reference voltage. The reference voltage is adjusted so that the final output from a differential amplifier is zero voltage at  $0^{\circ}\text{C}$  and 1000 mV at  $50^{\circ}\text{C}$  giving  $20\text{ mV}/^{\circ}\text{C}$  linear temperature response. Figure 7 gives the circuit diagram for the soil temperature sensor.

A timer circuit is used so that each level is sensed for 15 seconds and the reference voltage for 30 seconds. Thus, all the levels and the reference level are sensed and recorded in 120 seconds and the cycle is repeated. The analog output is recorded on a 6-channel Yokogawa recorder <sup>(1)</sup>. The outputs are identified in sequence beginning with the reference voltage and then 10 cm above surface, surface, 10, 20, 30 and 60 cm below the surface. The temperature can be read from the analog record with a resolution of  $0.5^{\circ}\text{C}$ . Figure 8 shows the variations in the soil temperature at the surface, 10, 20 and 30 cms below the surface. The soil heat flux has been computed using the temperatures at the surface and 10 cm below the surface <sup>(1)</sup>.

### 3.5 Net Radiometers

For observing the net all wave radiation,  $Q_N$ , a net pyrrometer supplied by India Meteorological Department, (spectral range :  $0.29 - 50\ \mu\text{m}$ ), was mounted on a 1.6 m tower. The output is directly in voltage form and an output of 1 mV corresponds to  $35.64\text{ watts}/\text{m}^2$ . This is utilized for estimating  $Q_N$  in the energy balance equation.

For computing the net short wave radiation,  $R(S)$ , two pyranometers (spectral range:  $0.4 - 1.1 \mu\text{m}$ ), were mounted back to back on the same tower and adjacent to the net pyrrometer, such that one sensor facing upward senses the short wave incoming radiation and an inverted one senses the short wave radiation reflected from the surface. The sensors manufactured by Licor-Inc. (USA), give a direct voltage output with  $1 \text{ mV}$  corresponding to  $100 \text{ watts/m}^2$ . The outputs of the three radiometers are recorded on an analog 6-channel Yokogawa strip chart recorder. The data is read with a resolution of  $0.2 \text{ mV}$  for the net radiometer and  $0.1 \text{ mV}$  for the pyranometers. The difference  $Q_N - R(S)$  gives the net long wave radiation,  $R(L)$ .

### 3.6 Flux plates

The heat flux at the surface was measured with the help of a flux plate manufactured by M/s International Thermal Instruments Co. (ITI), USA. It is a flat plate ( $2" \times 2"$ ) transducer made of polyimide-glass. The upper and lower plates of the transducer are in thermal contact with a miniature thermopile. When the plate is kept in contact with any surface the temperature difference across it produces a signal directly proportional to the heat flux. This signal output (in millivolts) multiplied by a calibration constant,  $k$  (supplied by the manufacturer), gives the heat loss or gain from the surface directly. To avoid radiative and convective errors the flux plate is exposed  $10 \text{ mm}$  below the soil surface. For this sensor an output of  $1 \text{ mV}$  corresponds to  $24.16 \text{ watts/m}^2$ . A similar flux plate with an output of  $1 \text{ mV}$  corresponding to  $25.74 \text{ watts/m}^2$  was placed at the surface to

monitor the variation of soil flux with respect to the surface wind.

An indigenous flux plate was designed using two brass plates and perspex as the interspersed material. This flux plate was calibrated with the 'ITI' flux plate and was field tested for its feasibility as an economical substitute. The output of these three sensors were also recorded on 6-channel Yokogawa strip chart recorder. On calibrating the indigenous flux plate with the ITI flux plate placed 1 cm below the surface, the calibration constant  $k$  was calculated as  $k = 0.45$  and an output of 1 mV corresponds to  $4.5 \text{ W/m}^2$ . Figure 9 shows the observations taken with the two flux plates placed 1 cm below the surface.

### 3.7 Propeller anemometer near the land surface interface

To monitor the effect of wind on the surface flux at the land surface interface, a Gill propeller anemometer was mounted near the flux plate at a height of 30 cm from the ground surface. The propeller has a vane arrangement on the rear side. Thus with the help of vane, the propeller anemometer always faced the incoming wind. The variations in the wind speed are directly obtained in voltage form. The propeller anemometer has a linear response upto 500 mV corresponding to 9.1 m/s (0 to 1800 rpm). This analog output is also recorded on the Yokogawa strip chart recorder.

### 3.8 Sonic anemometer

A 3-axis sonic anemometer, manufactured by M/s Applied Technologies Inc. (USA), was mounted on a 5.2 m high tower <sup>(2)</sup>, to measure the wind components along the three orthogonal axes



(u,v, w) and the temperature. The sensors contain ultrasonic 4 mm dia microphones which are energized by 200 khz sound pulses. Each axis has 2 such transducers separated by a pathlength of 15 cms. The data were recorded directly through RS-232 port on floppies at 10 cycles/sec rate for 15 minutes duration, at every hour.

Sonic anemometer data have been utilized to evaluate fluxes by the eddy correlation technique which requires fast response sensors. Figure 10 shows the 1 sec averaged kinematic fluxes of momentum and heat,  $u'w'$  and  $w'T'$  computed using the sonic anemometer.

### 3.9 Gill Propeller Anemometer

A 3-axis Gill propeller anemometer (19 cm dia) manufactured by M/s R M Young Co. (USA) was mounted on a 5.2 m high tower to measure the 3 components of wind i.e. u, v and w. The distance constant of this anemometer is 0.8 m. The output voltage varies linearly upto 500 mV corresponding to 9.1 m/s (1800 rpm). Two days data were recorded on floppies through a data logger at 10 cycles/sec every 3 hours (for 5 mins duration). Figure 11 shows the kinematic momentum flux,  $u'w'$ , obtained from the 3-axis Gill propeller anemometer, with the data averaged over 1 sec. The data collected are analysed separately for comparison with the sonic anemometer.

## 4. RESULTS AND DISCUSSION

The experimental set up described above can be used for studying land surface - atmosphere interactions on various time scales. The data collected will also be utilised separately for making turbulence studies, estimation of fluxes by eddy-

correlation technique and spectra of wind components near the surface. The preliminary results of the study of the heat exchange at the surface are discussed below.

#### (1) Heat and soil flux variations

The changes taking place at the surface depend on the type of surface, the atmospheric conditions and the radiant energy received by the surface <sup>(3,4)</sup>. The net radiation,  $Q(N)$ , received at the surface is the sum of net short wave,  $R(S)$  and the net long wave radiation  $R(L)$ . Figure 12 shows the variation of the **three** components for a day. The positive values indicate incoming radiation towards the surface whereas the negative values indicate radiation going away from the surface. As normally observed, it is seen that during the daytime, the net shortwave gain by the surface is more than the net longwave loss. At night, as there is no incident short wave radiation, the net radiation is equal to the net longwave radiation loss from the surface.

Figure 13 shows the soil temperature contours for a day, which conform to the pattern usually observed. During the daytime, the rate at which solar energy is incident is more than its rate of dissipation. As a result, the accumulated heat causes the surface temperature to rise. The diurnal variation of temperature recorded at the surface is followed by the lower layers with an exponential decrease in amplitude. There is also a lag in the time at which the maximum temperature is recorded at the successive layers when compared to surface maxima and this lag increases with depth <sup>(4)</sup>. Figure 14 shows a three

dimensional plot of soil temperature as a function of depth and time. The reduction in amplitude with depth and the lag of maxima (5) are clearly brought out .

The ground surface experiences diurnal temperature variations of nearly  $25 - 30^{\circ} \text{C}$ . This reduces with depth and is about  $1^{\circ} \text{C}$  at 30 cms below the surface.

The surface soil heat flux is highly varying and changes with various factors including wind and temperature. Figure 15 shows the dependence of the surface soil heat flux with surface temperature and wind during day and night. During the day (0900-1000 hrs), as shown in Figure 15 a, for an increase in the surface wind speed there is a fall in the surface temperature which in turn causes a reduction in the heat flux into the ground. Conversely, a decrease in the wind speed raises the surface temperature thus causing an increase in the downward heat flow. However, at night (2100-2210 hrs), as shown in Figure 15 b, the reverse takes place. An increase in wind speed causes a cooling in the surface temperature and hence an increase in the upward flow of the surface soil heat flux while a decrease in wind speed increases the temperature and causes a fall in the upward heat flux. It is also observed that the soil heat flux 1 cm below the surface, (Figure 15 c), follows the surface trend but with a lag of about 20 minutes.

The temperature profiles have been plotted for the levels, just above and below the soil surface, at different times of the day. These are similar to those usually observed near the ground

(4) surface and are shown in Figure 16.

(2) Energy balance equation

Considering the energy balance at the land surface interface, the energy balance can be written as:

$$Q_N = Q_H + Q_E + Q_G \quad \text{where}$$

$Q_N$  is the net all wave radiation,  $Q_H$  is the turbulent transfer of sensible heat into the atmosphere,  $Q_E$  is the contribution of the latent heat of evaporation and evapo-transpiration and  $Q_G$  is the transfer of heat through the ground (6).

Using the temperature (dry and wet-bulb) and wind speed data at 30cm and 160 cm, the surface fluxes of sensible heat and latent heat are evaluated by the profile technique. Under neutral conditions, the flux-gradient equations are :

$$\text{Sensible heat flux} = Q_H = -\rho C_p k^2 z^2 \left( \frac{\Delta \bar{u}}{\Delta z} \cdot \frac{\Delta \bar{T}}{\Delta z} \right)$$

$$\text{Latent heat flux} = Q_E = -\rho L_v k^2 z^2 \left( \frac{\Delta \bar{u}}{\Delta z} \cdot \frac{\Delta \bar{q}}{\Delta z} \right)$$

where  $\rho$  is the density,  $C_p$  is the specific heat at constant pressure,  $L_v$  is the latent heat of vapourization,  $k$  is the Von Karman constant and  $z$  is the height.

For evaluating the fluxes under non-neutral conditions, the equations are multiplied by the dimensionless stability factor :

$$(\phi_m \phi_x)^{-1} \quad \text{where} \quad \phi_x = \phi_w \text{ or } \phi_H$$

$$\text{For stable conditions } (R_i \text{ positive}) : (\phi_m \phi_x)^{-1} = (1 - 5 R_i)^2$$

$$\text{For unstable conditions } (R_i \text{ negative}) : (\phi_m \phi_x)^{-1} = (1 - 16 R_i)^3$$

where  $R_i$  is the Richardson Number,  $\phi_H$ ,  $\phi_w$  and  $\phi_m$  are the dimensionless stability functions for heat, water vapour and momentum.

The equations are thus :

$$\text{Sensible heat flux} = Q_H = -\rho C_p k^2 z^2 \left( \frac{\Delta \bar{u}}{\Delta z} \cdot \frac{\Delta \bar{T}}{\Delta z} \right) (\phi_m \phi_H)^{-1}$$

$$\text{Latent heat flux} = Q_E = -\rho L_v k^2 z^2 \left( \frac{\Delta \bar{u}}{\Delta z} \cdot \frac{\Delta \bar{q}}{\Delta z} \right) (\phi_m \phi_w)^{-1}$$

The soil heat flux  $Q_G$  is obtained from the temperatures at the surface and 10 cm below the surface, and the net radiometer gives the net radiation  $Q_N$ .

Figure 17 shows the variation of the energy balance components over a day, for 20 May 1992. On account of the strong heating of the ground, the sensible heat flux is high, and as there is meagre soil moisture, the latent heat flux is low.

Table 1 gives the hourly values of the different fluxes. It is observed that the energy fluxes are not balanced at each hour interval but when considered for the full day the energy is fairly well balanced (6).

## 5. SUMMARY

In order to study the energy exchange taking place at the earth's surface, an experimental set-up is designed. The instrumentation facility compatible with the automatic data logging system has enabled data to be monitored continuously. This experimental set-up can be utilized to study the temperature variations, the sensible and latent and the soil heat flux. Also, utilizing these and the net radiation data, the energy balance near the land surface - atmosphere interface could be studied.

## REFERENCES

- (1) Pillai J S, Sangeeta Saxena and K G Vernekar, 'A six level automatic soil temperature measuring system', communicated to Mausam, 1991.
- (2) Kaimal J C, 'Sensors and techniques for the direct measurement of turbulent fluxes and profiles in the atmospheric boundary layer', Atmos. Tech., No. 7, Fall 1975, pp 7-14.
- (3) Oke T R, 'Boundary layer climates', 1987, Methuen & Co., Ltd., London.
- (4) Rosenberg N J, B L Blad, S B Verma, 'Microclimate - The Biological Environment', 1983, John Wiley & Sons Inc., New York.
- (5) Campbell G S, 'An introduction to Environmental Biophysics', 1977, Springer - Verlag New York Inc.
- (6) Mitsuta Y, T Hanafusa, O Tsukamoto, H Kamanishi, 'A study of the energy budget at the air - ground interface', Bull. Diab. Prev. Res. Inst. Kyoto Univ., Japan, 1973, Vol. 22, part 4, No. 209.

TABLE 1  
-----  
20 MAY 1992  
-----

TIME Hrs.	NET RADIATION (R) (W/sq.m)	SENSIBLE HEAT FLUX (W/sq.m)	LATENT HEAT FLUX (W/sq.m)	SOIL HEAT FLUX (W/sq.m)
0100	-84	0	19.49	-66.5
0200	-77	-2.41	0.34	-70.0
0300	-77	-5.81	1.65	-66.5
0400	-77	-4.15	8.05	-66.5
0500	-70	-32.1	2.88	-66.0
0600	-63	-15.34	1.81	-66.0
0700	28	19.23	6.77	-31.5
0800	182	85.06	30.56	7.0
0900	322	134.63	58.72	45.5
1000	434	227.77	59.28	78.75
1100	476	236.75	77.19	112.0
1200	511	175.87	80.94	115.5
1300	497	188.84	82.37	147.0
1400	441	237.61	123.6	136.5
1500	364	219.11	154.4	108.5
1700	112	80.99	56.0	38.5
1800	-28	51.16	111.4	-7.0
1900	-91	4.78	19.58	-45.5
2000	-91	5.3	18.81	-56.0
TOTAL	2709	1607.92	+ 913.84	+ 247.45
			=	2769.21



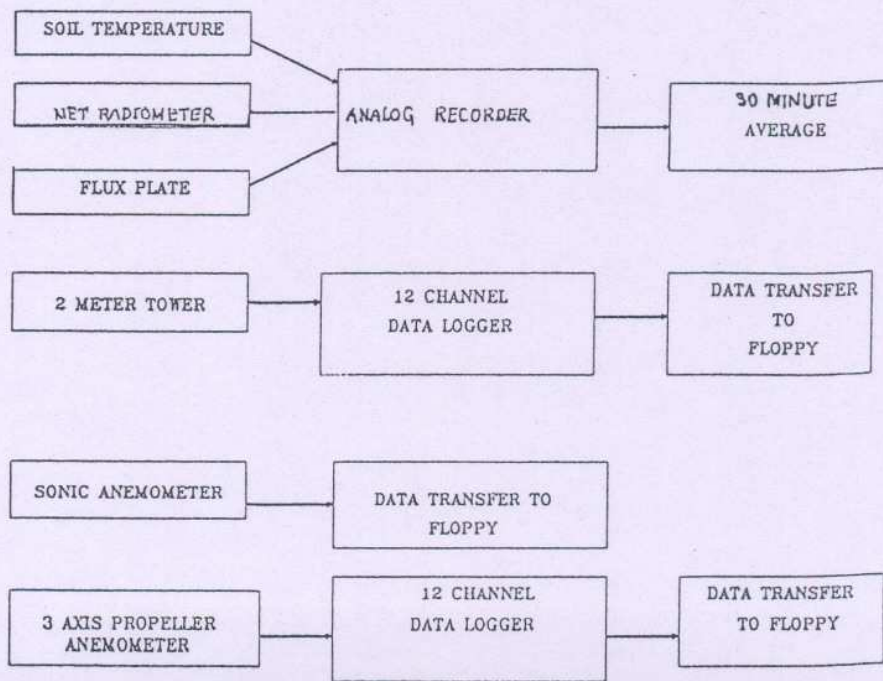
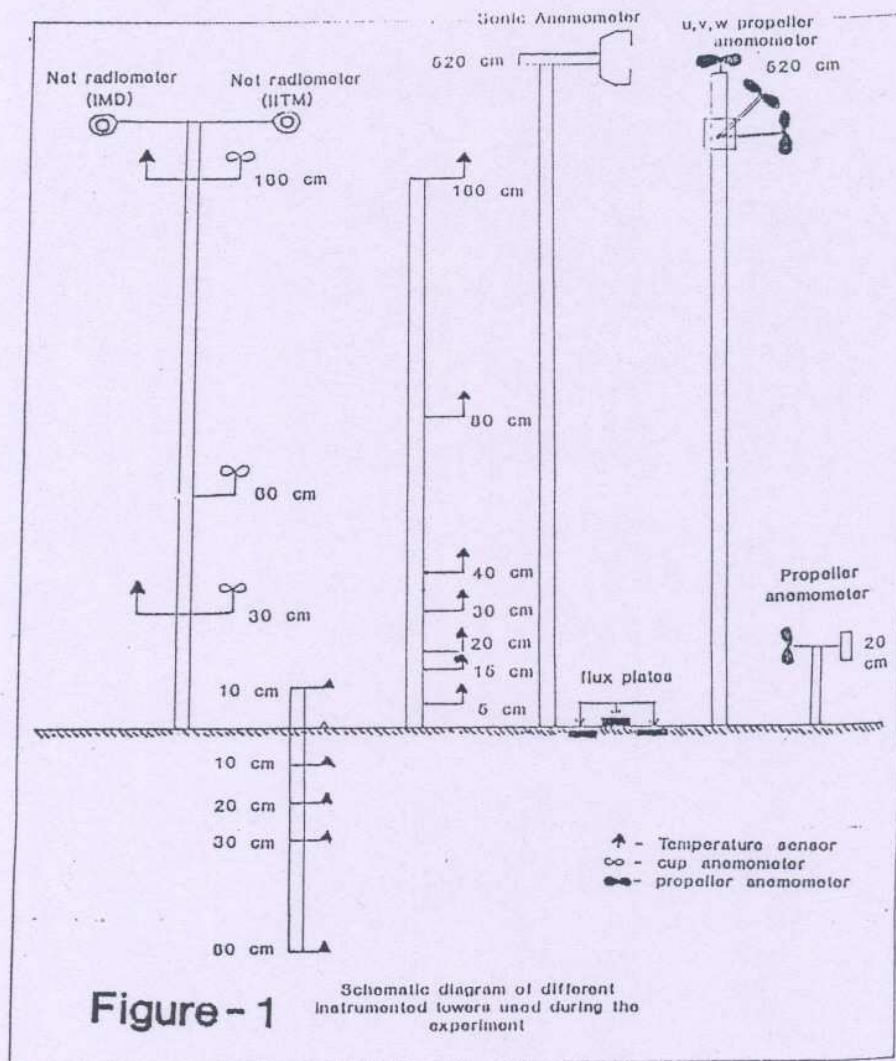


**Figure - 2**

DATA ACQUISITION SET UP FOR VARIOUS SENSORS

20 MAY 1992

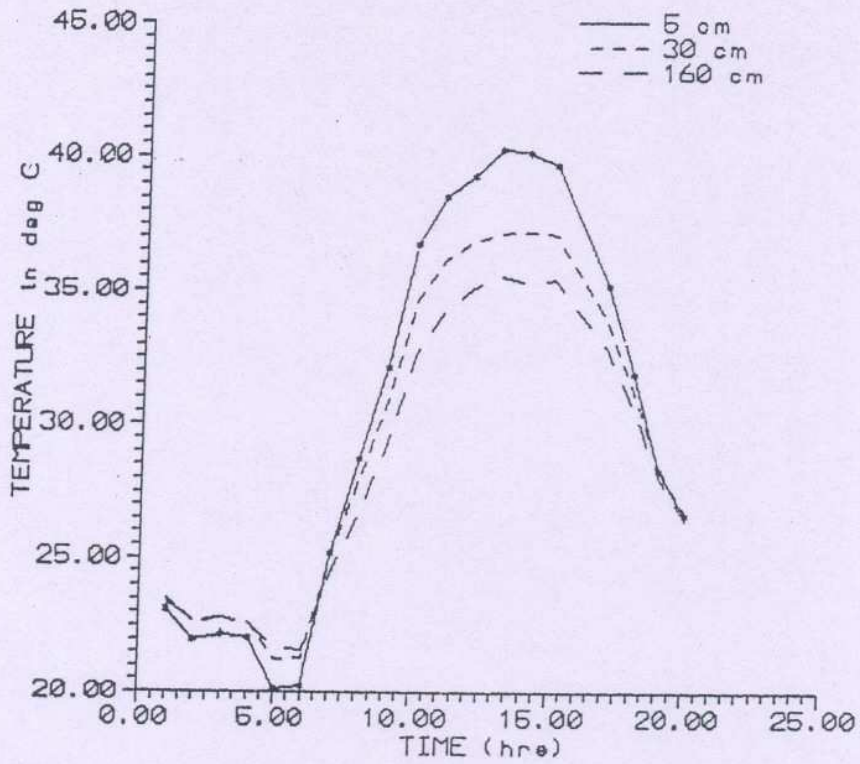


Figure-3

20 MAY 1992

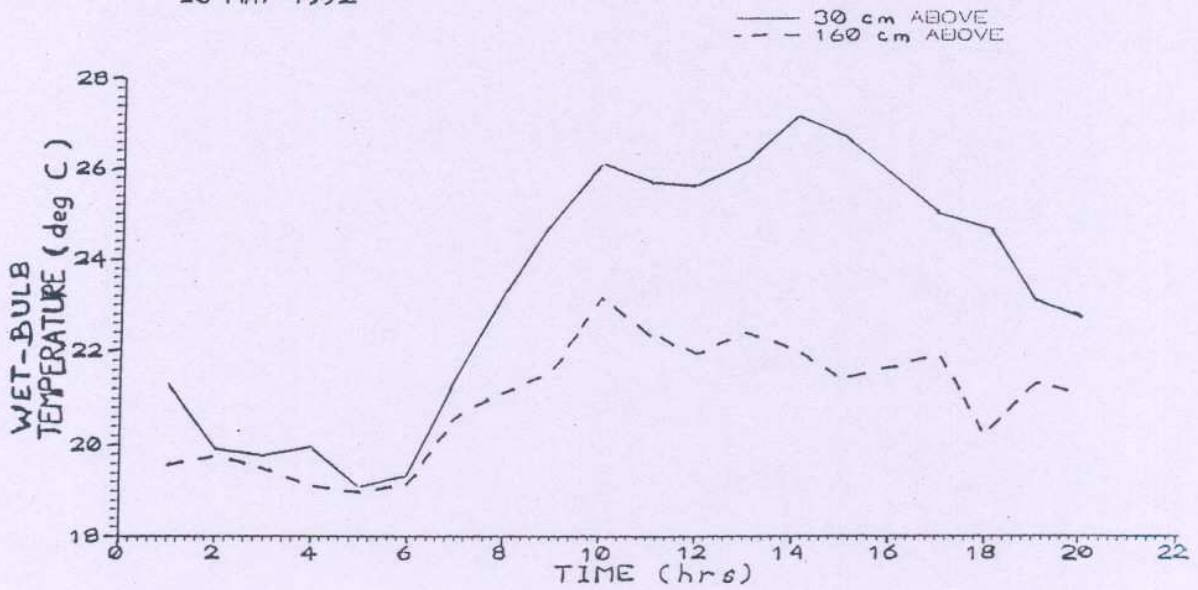
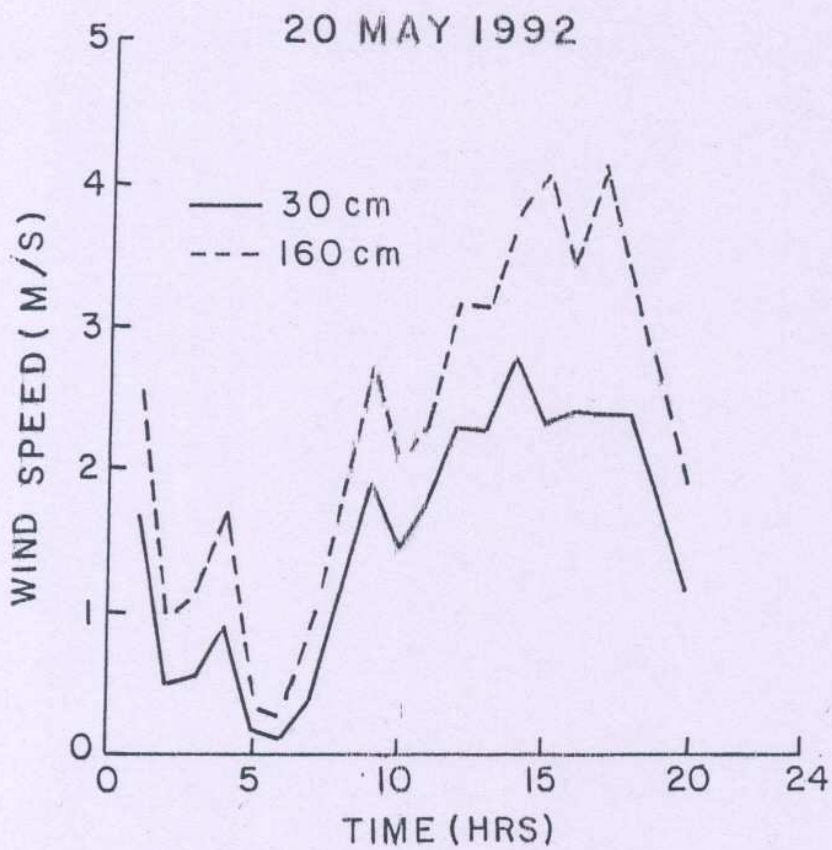
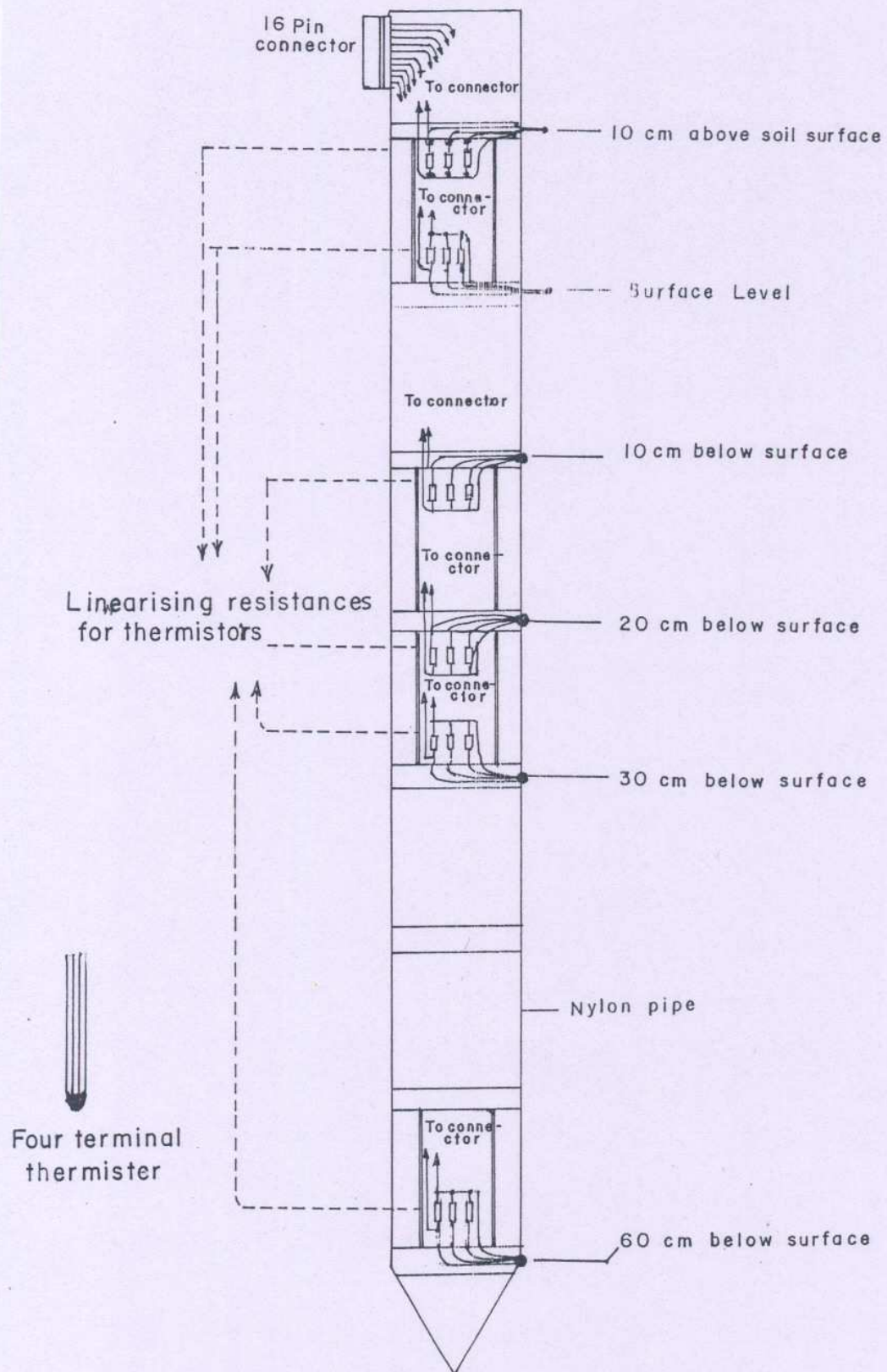


Figure-4



WIND SPEED VARIATIONS AT TWO LEVELS

Figure - 5



Cross section of the soil temperature probe

Fig. 6 .

Vcc = +9 V  
 CND = 0 V

RT1-RT6

RI-R7

R9-R12

Rref

R13

R14

R15

R16

CI-C6

C7

C8

C9

IC1

IC2

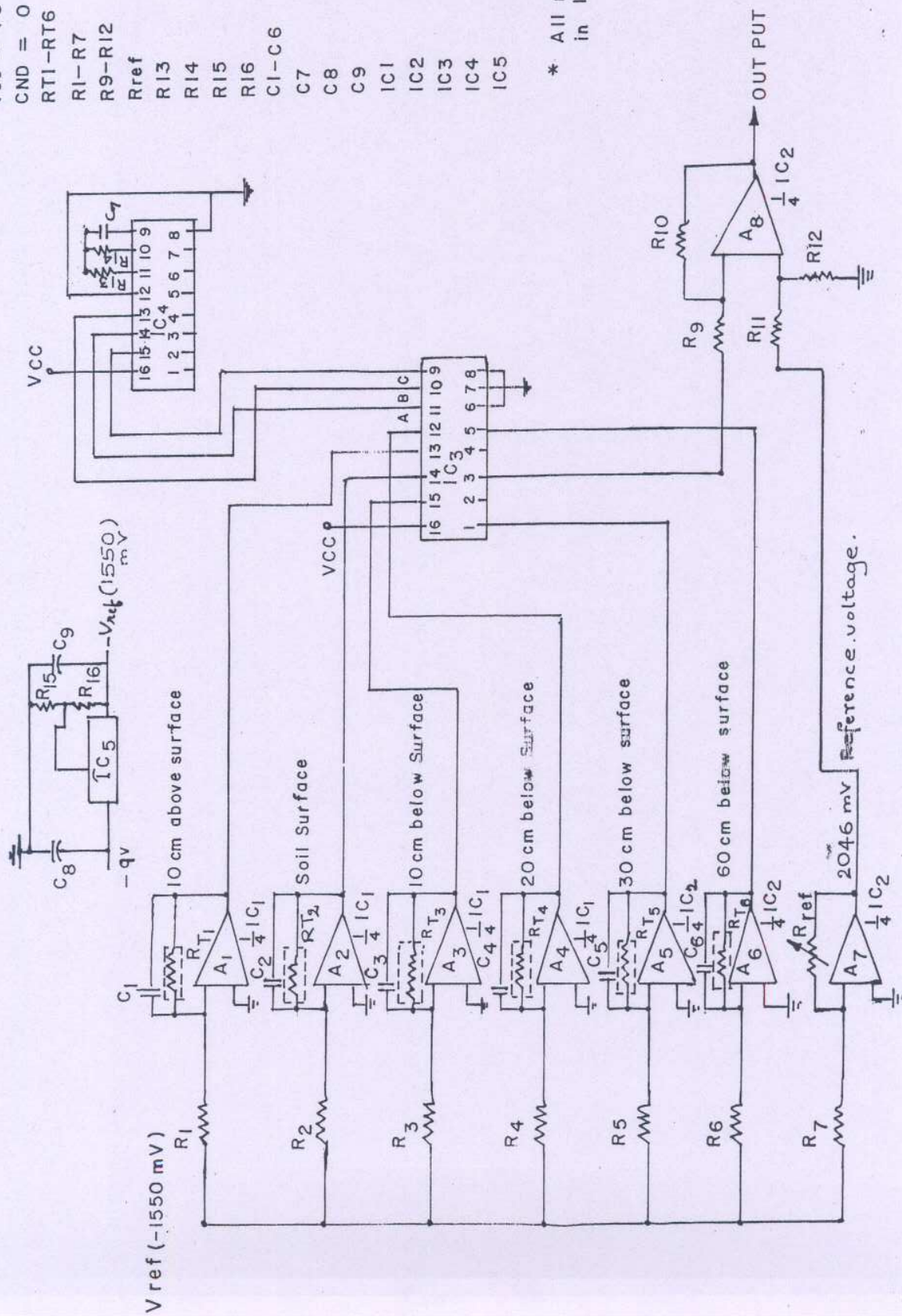
IC3

IC4

IC5

Thermistors  
 10 k $\Omega$   
 1 M $\Omega$   
 15 k $\Omega$  (var)  
 2.2 M $\Omega$   
 220 k $\Omega$   
 1 k $\Omega$  (var)  
 120  $\Omega$   
 0.1  $\mu$ F  
 0.22  $\mu$ F  
 1  $\mu$ F  
 10  $\mu$ F  
 LM 324  
 LM 324  
 CD 4051  
 CD 4060  
 LM 337

\* All resistors are in 1% Tolerance



Circuit diagram

Fig.7.

SOIL TEMPERATURE  
20 MAY 1992

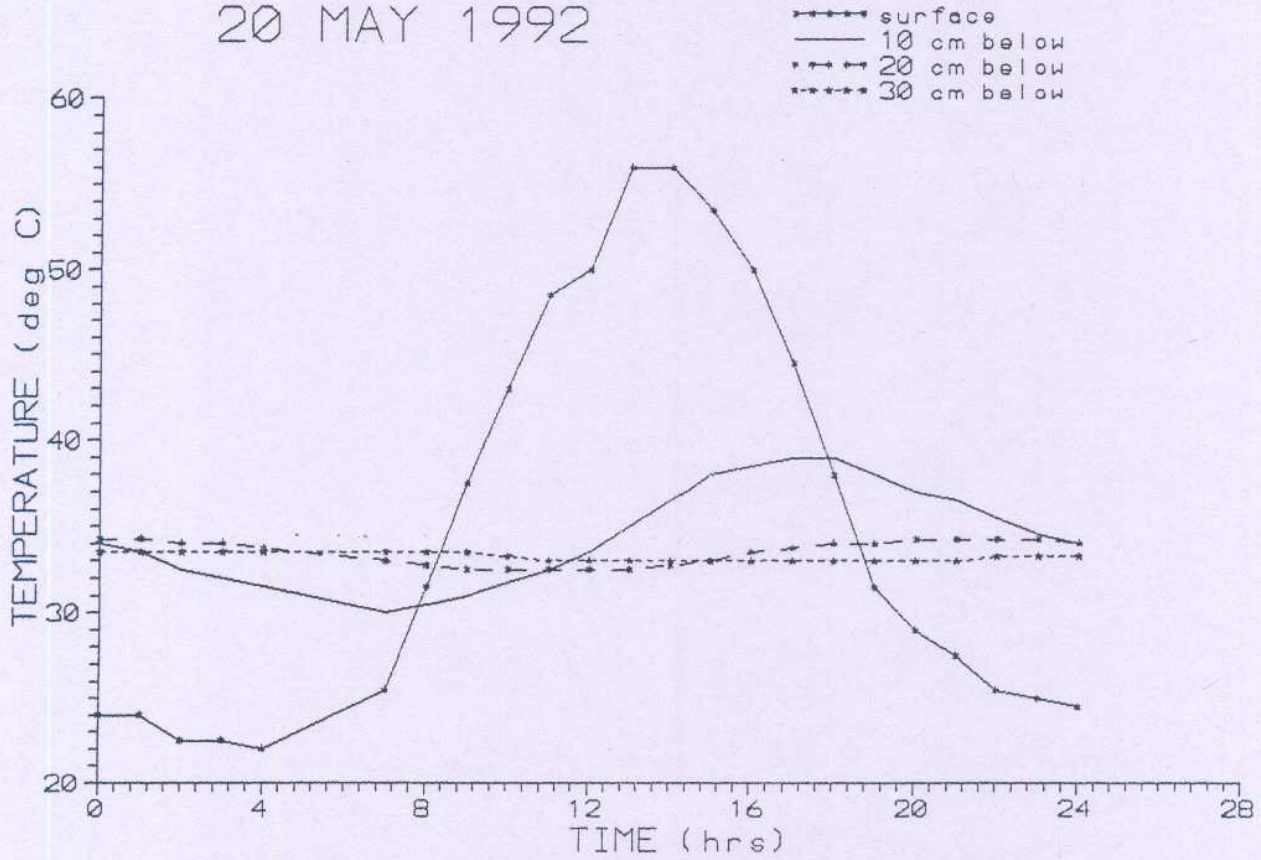
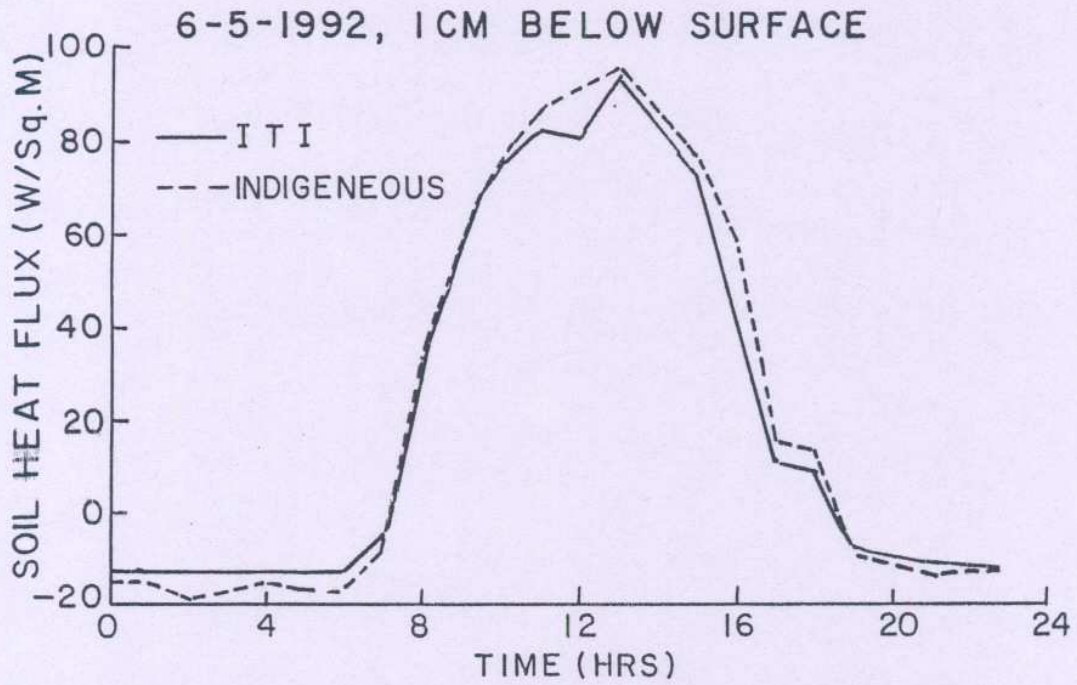
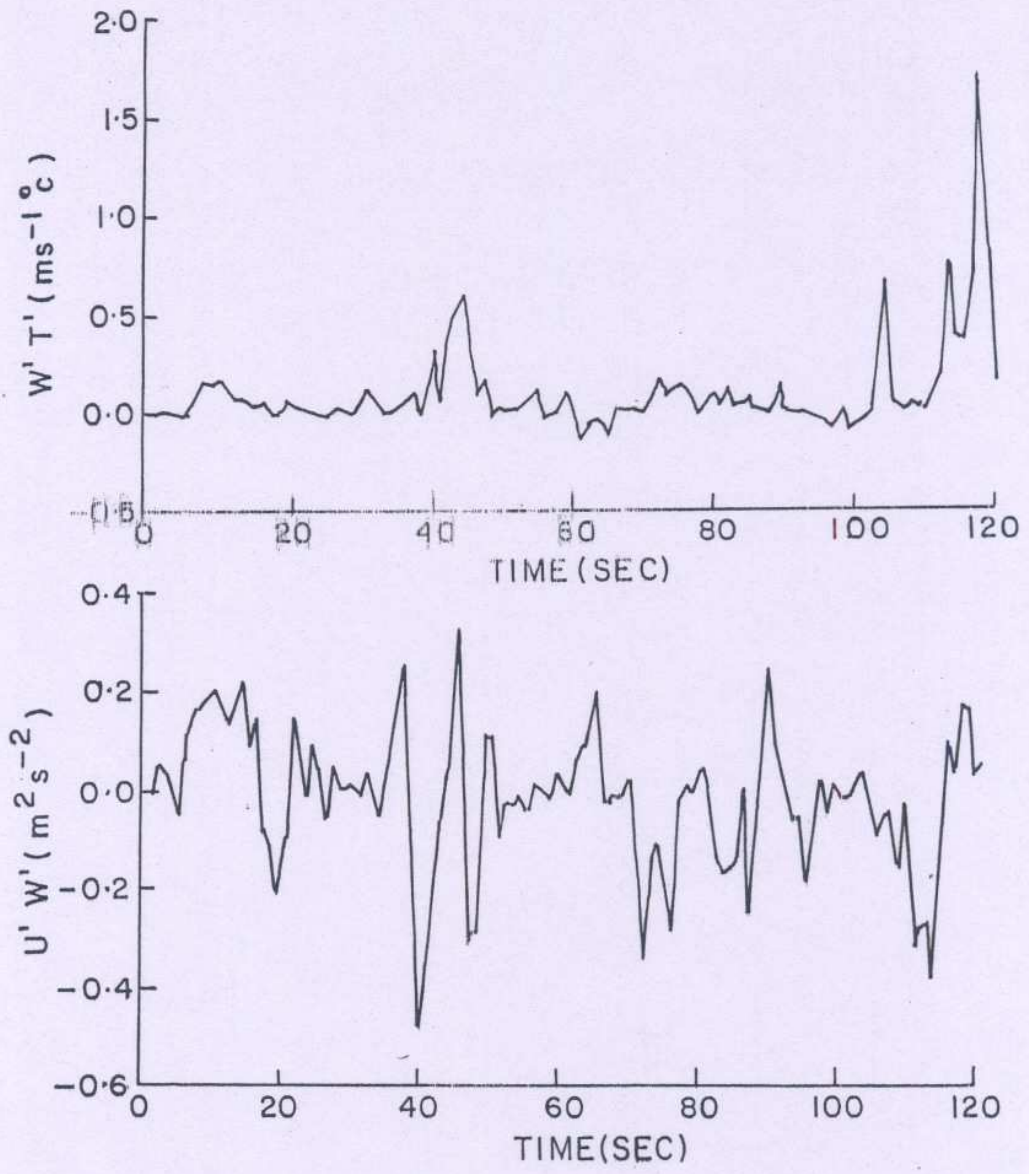


Figure -8



OBSERVATIONS USING INDIGENEOUS AND IMPORTED  
FLUX PLATES.

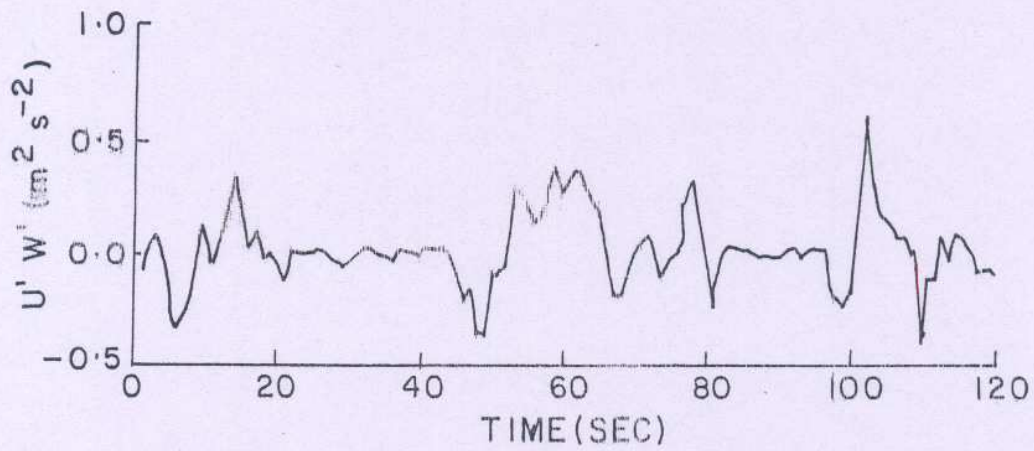
Figure - 9



KINEMATIC HEAT AND MOMENTUM FLUXES OBTAINED FROM SONIC ANEMOMETER

Figure - 10





KINEMATIC MOMENTUM FLUX OBTAINED FROM  
3 AXIS PROPELLER ANEMOMETER.

Figure-11

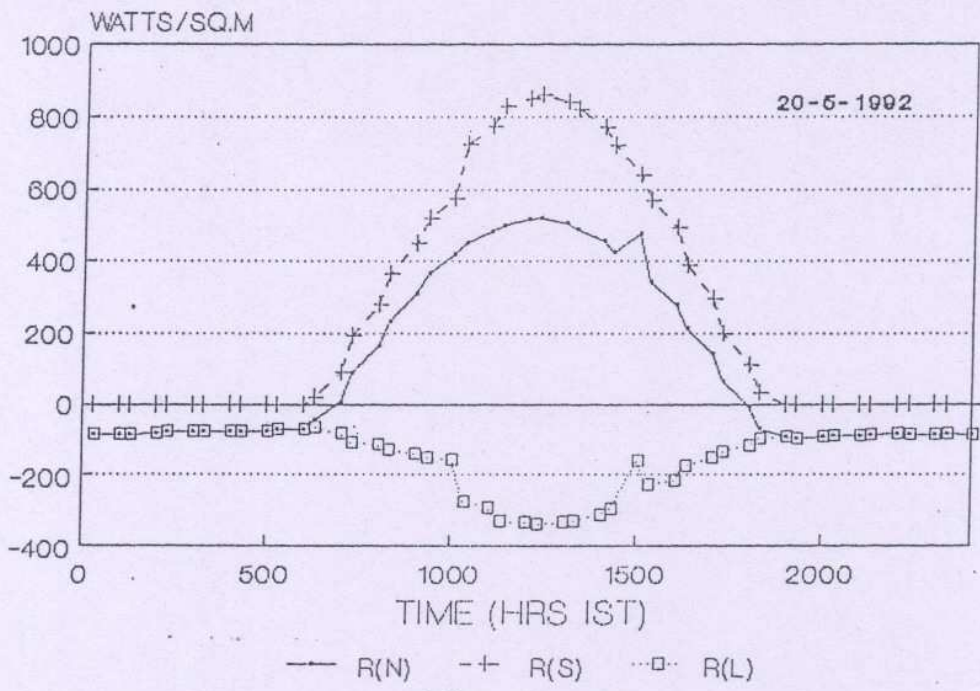


Figure - 12

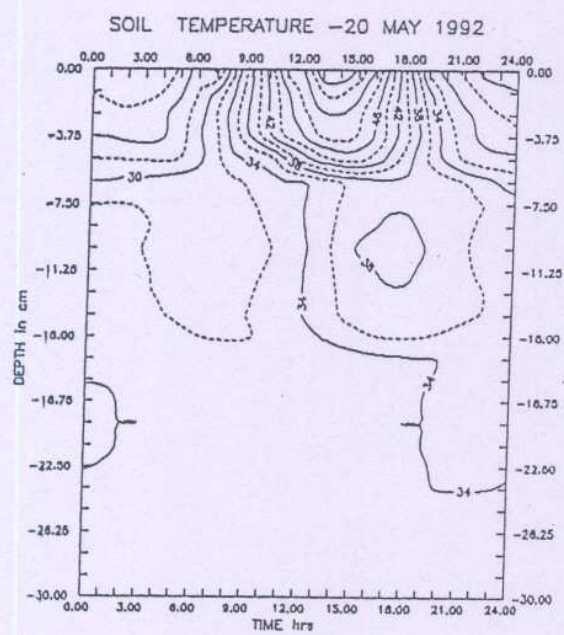
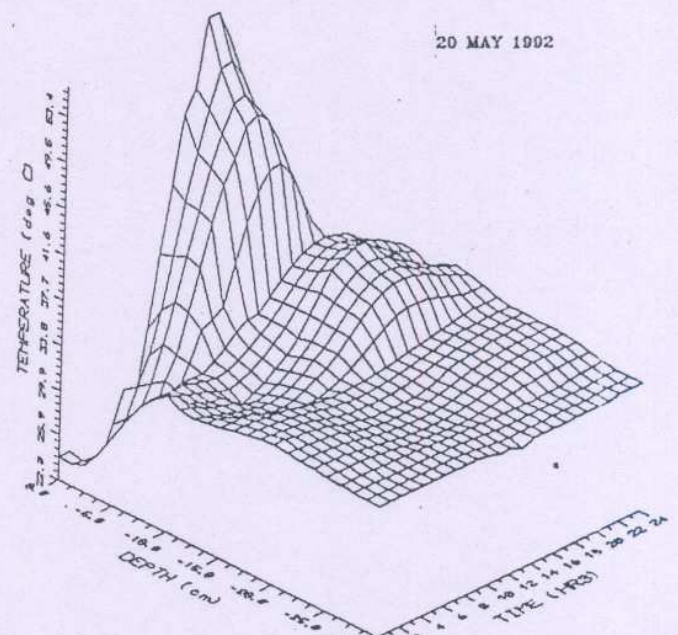
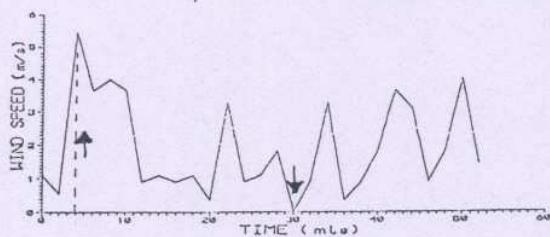


Figure - 13

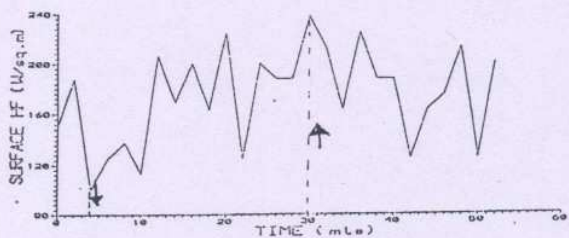
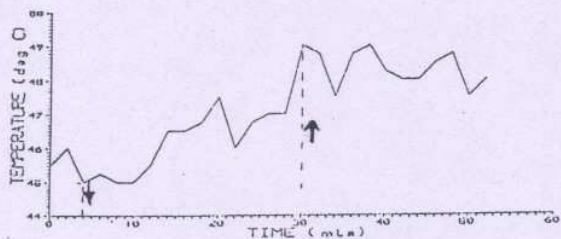


SOIL TEMPERATURE  
Figure - 14

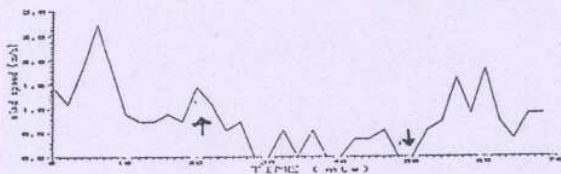
19 MAY 1992  
0000 hrs-1000 hrs



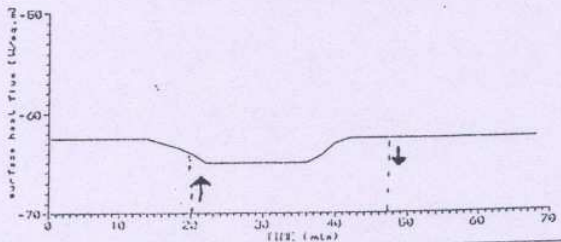
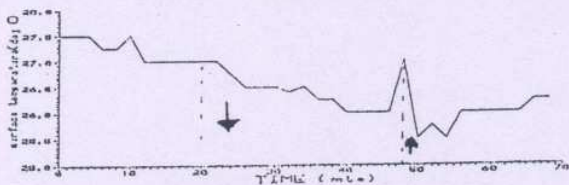
A



19 MAY 1992  
2100 hrs-2210 hrs



B



C

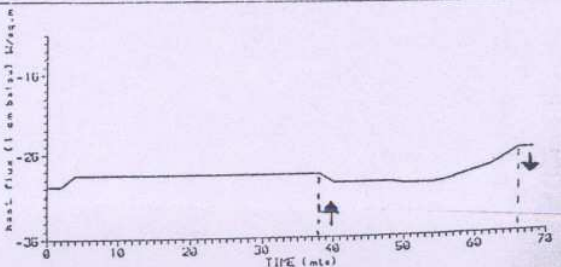


Figure-15

20 MAY 1992

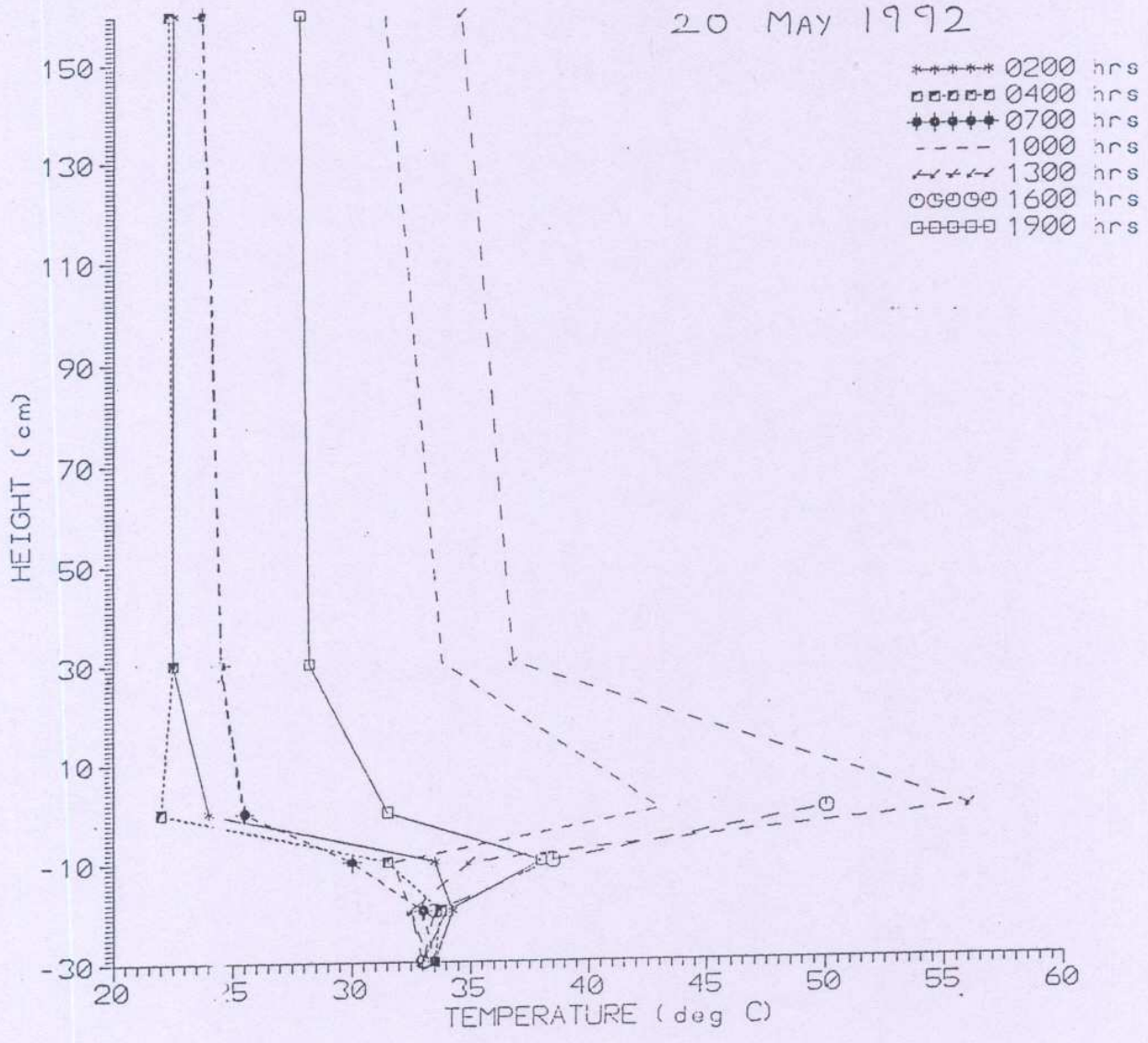


Figure - 16

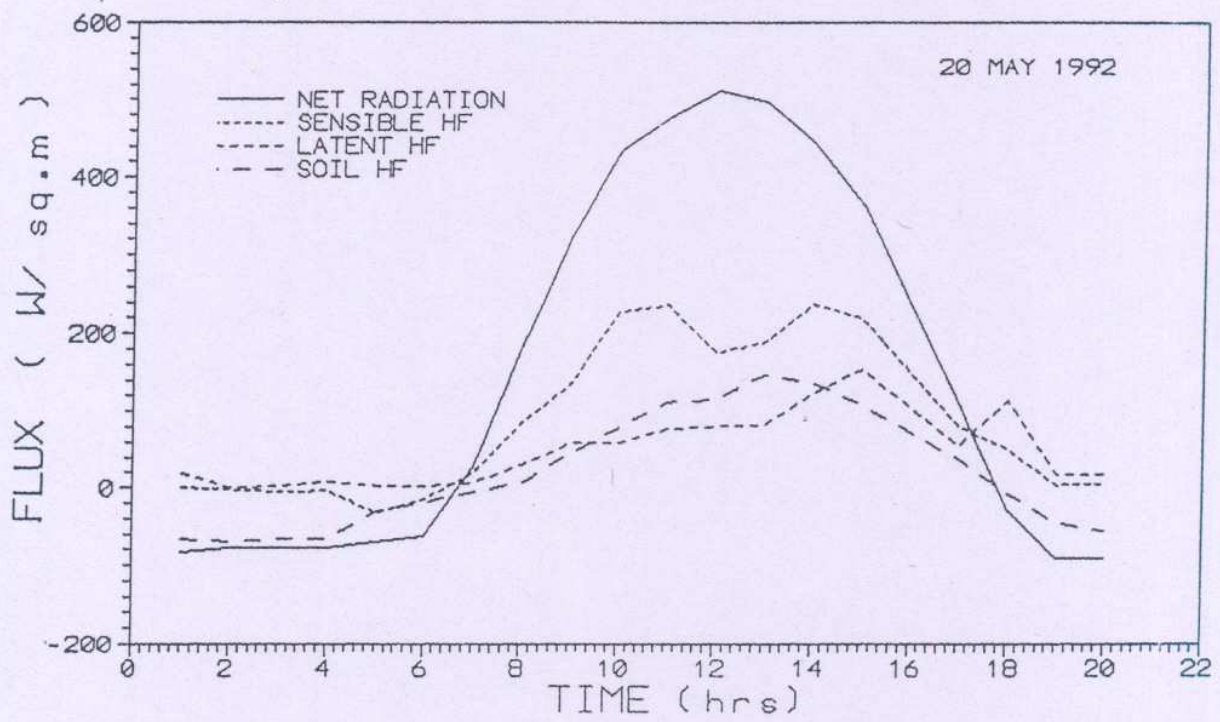


Figure-17